(43) Krigbaum, W. R. J. Am. Chem. Soc. 1954, 76, 3758.
(44) McIntyre, D.; Wims, A.; Williams, L. C.; Mandelkern, L. J. Phys. Chem. 1962, 66, 1932.
(45) Cantow, H. J. Z. Phys. Chem. (Frankfurt) 1956, 7, 58.
(46) Orofino, T. A.; Mickey, J. W., Jr., J. Chem. Phys. 1963, 38, 2512.
(47) Strazielle, C.; Benoit, H. J. Chim. Phys. Phys.—Chim. Biol. 1961, 58, 678.

Probe Diffusion in Solutions of Long-Chain Polyelectrolytes†

George D. J. Phillies* and Craig Malone

Department of Physics, Worcester Polytechnic Institute, Worcester, Massachusetts 01609

Kathleen Ullmann

University of Michigan, Ann Arbor, Michigan 48109

Gregory S. Ullmann

Department of Computer Science, University of Michigan, Ann Arbor, Michigan 48109

James Rollings and Li-Ping Yu

Department of Chemical Engineering, Worcester Polytechnic Institute, Worcester, Massachusetts 01609. *Received April 30, 1986*

ABSTRACT: Light-scattering spectroscopy was used to measure the diffusion of polystyrene latex spheres through solutions of partially neutralized poly(acrylic acid), as a function of polymer concentration, pH, ionic strength, and probe radius. D/D_0 follows a stretched exponential form $\sim\exp(-ac^{\nu}I^{\beta}R^{\delta})$, with $\nu \simeq 0.5$–1 (depending on I), $\beta \simeq -0.8$, and $\delta \simeq 0.2$, the last of these being substantially inconsistent with most theoretical models for probe diffusion. With partially (>50%) neutralized polymer, small (400 Å) probe particles diffuse much (up to eightfold) faster than predicted by the Stokes–Einstein equation; the validity of the Stokes–Einstein equation improves at higher ionic strength and for larger (up to 1.3 μm) probe particles.

Introduction

The diffusion of globular probe particles through polymer solutions is a phenomenon of considerable scientific and practical interest. The probe diffusion coefficient gives valuable information, different from that elsewise available, on polymer dynamics. Probe diffusion is a model for such scientific phenomena as inter- and intracellular transport in living tissues. Particle motion in polymer solutions may also occur during a variety of potentially practical circumstances, such as the production of long-chain polysaccharides by bacterial fermentation or the electrophoretic preparation of whole cells by free (unsupported) Tiselius electrophoresis.

We have previously reported studies on the diffusion of weakly charged probes (polystyrene latex spheres, serum albumin molecules) through aqueous solutions of poly(ethylene oxide),[1-3] poly(acrylic acid),[4-6] and bovine serum albumin.[7] In these systems, electrostatic forces between probe and polymer were relatively small: the polyacrylic acids studied by Lin and Phillies[4-6] were not neutralized. Since carboxylic acid groups are weak acids, in their work each polymer chain would have contained only a few ionized carboxylate groups. The serum albumin studies were all performed in 0.15 or 0.5 M NaCl, so electrostatic interactions in the serum albumin solutions were substantially screened.

In our previous work,[1-8] D usually followed a "stretched exponential" form

$$D/D_0 = \exp[-ac^{\nu}M^{\gamma}R^{\delta}] \quad (1)$$

where D_0 is the probe diffusion coefficient in pure solvent, c and M are the polymer concentration and molecular weight, and R is the probe radius. a, ν, γ, and δ are fitting parameters. Stretched exponential forms also describe the macroscopic viscosity η of our polymer solutions. Furthermore, one of us[9] has recently shown that the entirety of the published modern data on polymer and biopolymer self-diffusion in solution is accurately described by stretched exponential forms. We were therefore motivated to apply generalizations of eq 1 to the results described below.

The Stokes–Einstein equation has long been used to interpret the diffusion coefficients of spherical bodies in simple liquids, the usually-assumed condition for the validity of the Stokes–Einstein equation being that the probe radius R is much larger than the radius of any of the surrounding solvent molecules. Surprisingly, even with very large (R = 1.5 μm) probes, the Stokes–Einstein equation fails in some high-molecular-weight polymer solutions.[1-7]

We define the apparent hydrodynamic radius R_{ap} as

$$R_{ap} = \frac{k_B T}{6\pi\eta D} \quad (2)$$

the hydrodynamic radius R_0 measured in pure solvent by

$$R_0 = \frac{k_B J}{6\pi\eta D_0} \quad (3)$$

and the non-Stokes–Einsteinian interaction parameter as

$$K = R_{ap}/R_0 \quad (4)$$

Here k_B, T, and D_0 are Boltzmann's constant, the absolute temperature, and the diffusion coefficient in pure solvent, respectively. For spherical particles, eq 3 is the Stokes–Einstein equation. The probe radius R of eq 1 is identified with R_0. At large c, one finds[1-7] $K < 1$ (sometimes $K \ll 1$). Such obvious artifacts as polymer binding or probe

*To whom correspondence may be addressed.
†This work supported by the National Science Foundation under Grants CHE85-15852, CHE82-13941, and CPE83-11461.

0024-9297/87/2220-2280$01.50/0

aggregation due to probe–polymer incompatibilities lead to $K > 1$, not $K < 1$; the observation $K < 1$ seems to be a real effect. Indeed, in poly(ethylene oxide) solutions Ullmann and Phillies[1] were able to quantify separately the polymer adsorption and the non-Stokes–Einsteinian behavior of the probes.

We here report a study of probe diffusion in a system with strong electrostatic interactions. The probe particles were polystyrene latex spheres. The polymer was partially neutralized high-molecular-weight poly(acrylic acid) (PAA). The Debye screening length k_D was varied by addition of a mobile electrolyte.

The next section of this paper presents our experimental methods. Unlike our previous work, we obtained the complete molecular weight distribution $W(M)$ of our polymer. Measurements of D and $W(M)$ are given in the third section. Our complete numerical data appear as tables in the supplementary material. A final section compares our results with previous experiments on probe diffusion in polyelectrolytes and with theoretical models for probe diffusion.[10]

Experimental Methods

The polymer in these experiments was poly(acrylic acid) (PAA) (Poly-Sciences, Inc.), of nominal molecular weight 450 000, which had been partially or completely neutralized with NaOH. The pH of the neutralized PAA ranged from 4 to 10.7. We also studied probes in nonneutralized PAA, whose concentration-dependent pH went from 2.8 to 3.7 as c was varied. The solvent was deionized (14 MΩ) water. PAA concentrations extended from 0 to 20 g/L. The background electrolyte was NaCl, at concentrations of 0 to 0.1 M. Poly(acrylic acid) in solid form may contain significant amounts of water of hydration; PAA concentrations were determined by conductometric titration with NaOH. (Our solid PAA was found to contain 7 wt % water of hydration.) pK's of carboxylic acid groups are sensitive to the proximity of other fixed charges and hence can depend on polymer concentration, so the pH of each sample was given a (very small) final adjustment after bringing the sample to the desired concentration and ionic strength.

The molecular weight distribution of the polymer was determined with aqueous size-exclusion chromatography (SEC). Our SEC system was based on a Waters Associates M6000A solvent delivery system, U6K sample injector, and R401 differential refractometer. Linearity of molecular weight against elution volume was maintained by coupling a 450-mm TSK-65F column to a 225-mm TSK-40S Fractogel column.[11] Columns were loaded locally with a Micromeritics 705-A stirred slurry column packer, using a flow rate of 0.6 mL/min of 0.3 volume fraction resin/water slurry. Columns were eluted with degassed 0.5 M NaOH; all mobile phases were passed through 0.2-μm Fluoropore (Millipore) filters before entering the columns. At 0.08 mL/min flow, the column system had an efficiency of 3900 plates per meter (theoretical value, 4300 plates per meter[11]) by the procedure of Kato et al.[12] and Yau et al.[13] The differential refractometer was serially coupled to an on-line LDC/Milton-Roy KMX-6 low-angle laser light scattering detector,[14,15] incorporating a 2-mW HeNe laser and 6–7° (annular) scattering angle. dn/dc of the poly(acrylic acid) was 0.227 mL/g, as inferred from the integrated response of the differential refractometer, by comparison with dextran, by using the procedure of Yu et al.[16]

Analog data from both detectors were digitized and analyzed with the MOLWT3 software package (LDC/Milton-Roy) to obtain the concentration and weight-average molecular weight $(M_w)_v$ of each elution volume, as shown in Figure 9. Numerical integration of the $(M_w)_v$ curve gives the conventional molecular weight averages M_n, M_w, and M_z. Chromatographic dispersion is expected to lead to a small artifactual increase in these averages.[13]

The probe particles used in these experiments were carboxylate-modified polystyrene latex spheres, identical with those used in our previous work on probe diffusion in poly(ethylene oxide).[1,2] The nominal diameters of these spheres were 0.038 μm (Dow Pharmaceuticals, 0.296 mequiv of nominal surface charge/g of polymer), 0.12 μm (Polysciences, Inc., 0.92 mequiv of nominal surface charge/g of polymer), 0.7 μm (Polysciences, Inc., 0.46 mequiv of nominal surface charge/g of polymer), and 1.28 μm (Polysciences, Inc., 0.12 mequiv of nominal surface charge/g of polymer). From light-scattering spectra of dilute spheres in pure water, the apparent hydrodynamic radii of these spheres are 208 Å, 517 Å, 0.322 μm, and 0.655 μ, respectively. The sphere concentrations used in these experiments were 5×10^{-4} (w/v) for the 0.038-μm spheres and substantially less for the larger spheres. Most of our studies were made on the 0.038-μm spheres. At these concentrations, multiple scattering is negligible, while the sphere–sphere interactions studied by Gorti, Plank, and Ware[17] should be insignificant.

Diffusion coefficients were measured with quasi-elastic light-scattering spectroscopy. For most of the experiments, the light source was a 20-mW HeNe laser, light being passed through a short-focal-length lens into the sample cell. The sample cell was thermostated by mounting it in a large block of copper, through which temperature-controlled (± 0.05 K) water was continually passed. Possible hazards from convection were minimized by choosing working temperatures (18–24.9 °C) close to room temperature. The available scattering angle was 90°. Scattered light was isolated with a pair of small irises, and detected with an RCA 7265 photomultiplier tube. Correlation functions were accumulated with 64- or 144-channel Langley-Ford Instruments digital correlators, the spectral baseline being determined from delay channels in the correlator. Correlator sample times were selected so that the spectrum fell to half its initial value in 8 to 15 channels; with the 144-channel correlator, up 25 channels were allowed for this 50% decay. For the survey study of the q-dependence, a Spectraphysics 2020-03 Ar^+ laser operating on the 5145, 4880, and 4579-Å lines was used as a second light source.

Spectra were analyzed with Koppel's method of cumulants.[18] Each spectrum was fit separately to the truncated expansion

$$\ln [S(k,t) - B] = \sum_{i=0}^{N} K_i(-t)^i/i! \qquad (5)$$

using N values 1, 2, 3, 4, and 5. Here $S(k,t)$ is the measured spectrum, B is the measured base line, and the K_i are the cumulants. The best value of N (generally 2 or 3) were identifiable in that further increases in N, as to $N = 4$, did not lead to a significant improvement in the statistical quality of the fit. D was inferred from the first cumulant. Signal-to-noise ratios (defining the signal to be the extrapolation of $S(k,t) - B$ to $t = 0$ and defining the noise to be the root-mean-square error in the best fit to the spectrum) were in the range 250–500.

The interpretation of light-scattering spectra of complex systems is a difficult problem. As shown a decade ago by one of us[19,20] (see also Jones,[21] Kops-Werkhoven et al.,[22] and Lodge[23]), if the scattering spectrum $S(k,t)$ of a thermodynamically nonideal mixture is dominated by scattering from a single species and if that species is dilute, $S(k,t)$ yields a single diffusion coefficient D. Within experimental error, D is the single-particle (tracer) diffusion coefficient of the scattering species in a pseudobinary mixture, one component being the scatterers and the other pseudobinary component being the (perhaps complex) nonscattering part of the mixture.

The experiments reported here were performed in this limited domain in which the spectrum simplifies. Lin and Phillies[4–6] have previously shown—for the combinations of sphere and polymer concentrations employed here—that the light scattered by poly(acrylic acid) in water is negligible by comparison with scattering due to the polystyrene spheres. D, as obtained from the first spectral cumulant, is therefore identified with the spheres' self-diffusion coefficient.

Light scattering by the polymer could lead to either of two artifacts: (i) introduction of additional exponentials, reflecting polymer motion, into the spectrum of the mixture or (ii) unanticipated heterodyne detection, if the polymer served as a local oscillator. However, with the laser powers, acceptance angles, and integrating times used for the polystyrene sphere spectra, $S(k,t)$ of sphere-free polyacrylic acid has no perceptible time dependence (though such a dependence could be observed by increasing the laser power and integrating time). Furthermore, examination of known heterodyne spectra (as obtained by placing a glass-rod local oscillator in the scattering cell[4–6]) showed that the heterodyne and homodyne decay times of sphere/polymer

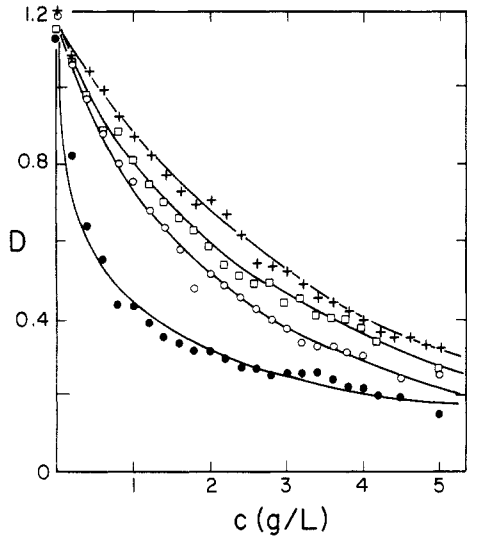

Figure 1. Diffusion coefficient of 0.038-μm polystyrene spheres at different polymer concentrations, in solutions containing various amounts of added electrolyte. D has units 10^{-7} cm^2/s; c is in g/L. Solution pH was 6, corresponding to 60% neutralization of the polymer. Ionic strengths were 0.0 M (filled circles), 0.01 M (open circles), 0.02 M (squares), and 0.10 M (crosses).

mixtures had the expected 2:1 ratio, so the polymer did not act as a local oscillator.

As an additional test for polymer scattering, we subtracted spectra of selected polymer solutions from spectra of sphere/polymer mixtures having the same polymer concentration. Such subtractions are correctly performed at the level of the field correlation function $g^{(1)}(t)$, not the intensity correlation function $g^{(2)}(t)$. Cumulant analysis of the resulting difference spectra showed that the subtraction did not change D significantly; i.e., the polymer contribution to $S(k,t)$ of the sphere/polymer mixture is not important. We thus have three experimental arguments that scattering by the polymer did not significantly perturb our spectra.

Cannon–Fenske and Ubbelohde viscometers were used to determine the viscosities of the polymer solutions at the working temperatures used to measure D. The viscometer bath temperature was stabilized to within 0.1 K. Small differences (<2 K) between different series of measurements were compensated by using the known temperature dependence of η of pure water. Indices of refraction were checked with a Bausch&Lomb Abbe-56 refractometer; n of our (very dilute) polymer solutions was always extremely close to the index of refraction of water.

Experimental data was fit to a series of algebraic forms, as discussed below, using a nonlinear least-squares fitting program given by Noggle.[24] The program, based on the simplex method, was rewritten by one of us for an ATT 6300 computer. The error in a measurement of D is a fraction of the absolute value of D, so the quantity minimized was the fractional difference

$$\sum_{i=1}^{N}[(D_i - T_i)/D_i]^2 \qquad (6)$$

between data points D_i and calculated points T_i, the sum passing over all N data points.

Results

We had access to a long series of potential experimental variables, including the polymer concentration c, solution pH and ionic strength I, probe radius R, polymer molecular weight M, and scattering vector q. A systematic study of all of these variables is beyond the scope of a single paper. Here the dependence of D on polymer concentration and solution ionic strength was observed in detail. Limited measurements were made with a variety of probe sizes at several different pH values. Changing the ionic strength alters the range of electrostatic interactions in solution. Changing the pH changes the fractional neutralization A,

Table I
Parameters from Nonlinear Least Squares Adjustments of the Stretched Exponential $D = D_0 \exp(\alpha c^\nu)$ to Measurements (Figure 1) of D against c at Fixed I

I	D_0	α	ν	rms error
0	1.17	0.99	0.42	7.6%
0.01	1.26	0.56	0.69	4.8%
0.02	1.135	0.36	0.85	3.4%
0.10	1.14	0.27	0.98	8.8%

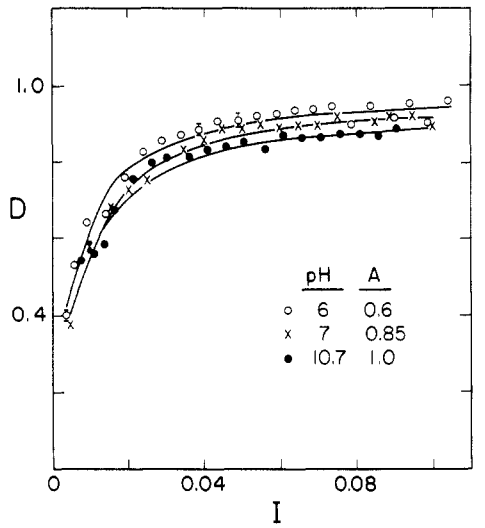

Figure 2. Diffusion coefficient of 0.038-μm polystyrene spheres in 1 g/L poly(acrylic acid), as a function of ionic strength, at pH values 6, 7, and 10.7, corresponding to fractional neutralizations A of 0.6, 0.85, and 1.0. D has units 10^{-7} cm^2/s. I includes both background electrolyte (NaCl) and sodium polyacrylate, treating the polyacrylate as univalent ions at the acrylic acid monomer concentration.

and hence the average charge, of the poly(acrylic acid) molecules. A brief survey was made of the q-dependence of the line width, finding no significant deviation (at c = 1 or 5 g/L, I = 0.0 or 0.1 M) from the expected q^2-proportionality, even when q^2 was varied nearly a factor of 2.

Effect of Polymer Concentration. Figure 1 shows the dependence on concentration of D of the 0.038-μm spheres at several ionic strengths: I_b = 0, 0.01, 0.02, and 0.1 M. Here I_b is the ionic strength of the background electrolyte, not including the sodium polyacrylate. The pH was 6, corresponding to a 60% neutralization of the polymer. Between 0 and 5 g/L, D falls by a factor of 4–5. At small I_b, the drop in D occurs largely at low c. At large I_b, D changes rather uniformly with increasing c. At fixed c, the diffusion coefficient always increases with increasing I_b. A numerical tabulation of this data is found in Tables 1–4 of the supplementary material.

The solid lines in Figure 1 indicate nonlinear least-squares fits of the data to a stretched exponential

$$D = D_0 \exp(-\alpha c^\nu) \qquad (6)$$

retaining D_0, α, and ν as free parameters. Each series of points is described extremely well by the equation, root mean square errors being 3–9%. Table I and Figure 10 give actual values for the fitting parameters. α falls nearly fourfold as the ionic strength is increased from 0 to 0.1 M, while ν perhaps doubles in the same ionic strength regime. α and ν are somewhat sensitive to D_0. For example, at I = 0.01 M, replacement of the best-fit value for D_0 with the measured value of D_0 changes α by 10%.

Effect of Background Electrolyte. Figure 2 (and supplementary material, Tables 5–7) shows D against ionic strength for the 0.038-μm probes at pH 6, 7, and 10.7, corresponding to A of 0.6, 0.85, and 1.0, respectively. I

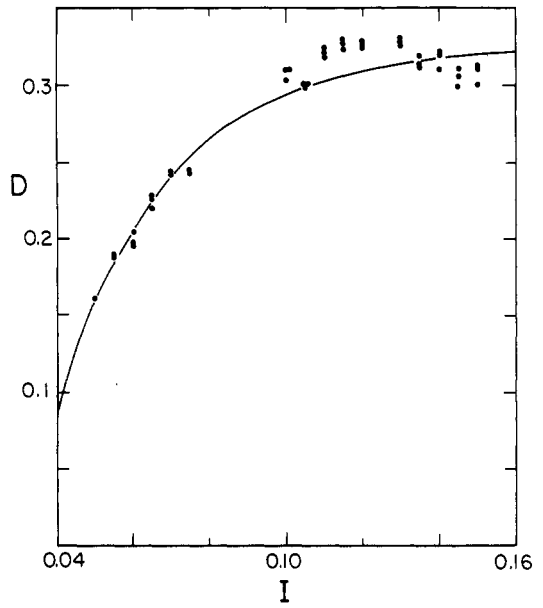

Figure 3. Diffusion coefficient of 0.038-μm polystyrene spheres in 5 g/L polymer, pH 6, at different ionic strengths. Other conditions as in Figure 2.

includes the sodium polyacrylate as well as the ionic strength I_b of the added electrolyte. The polymer concentration was 1 g/L. There is a clear plateau at high (>0.03 M) ionic strength. Reducing I from 0.03 M to its minimum value reduces D to less than half its initial value. Changing pH has but a small effect on D, D falling by less than 10% as pH is raised from 6 to 10.7 (equivalently, as A is increased from 0.6 to 1.0).

Figure 3 (supplementary material, Table 8) shows a similar study of D against I, at the higher polymer concentration 5.0 g/L. There is again a plateau in D at high ionic strength. D is halved as I is decreased from 0.15 M to its minimum. I_{pl}, the ionic strength at which the plateau occurs, increases with increasing polymer concentration, from I_{pl} = 0.03 M in 1 g/L polymer to I_{pl} = 0.1 M in 5 g/L polymer.

Solid lines in Figures 2 and 3 show fits to a stretched exponential

$$D/D_0 = \exp(-\alpha I^\beta) \quad (7)$$

β being a scaling exponent. The stretched exponential provides a good description of the I dependence of D at all ionic strengths and polymer concentrations. The numerical fitting parameters in Table II depend on the extent to which the sodium polyacrylate is assumed to contribute to I (see below). All treatments of I find $\beta < 0$.

The spectral line shape was studied systematically by varying the truncation of the cumulant expansion. All spectra were fit well with two or three cumulants, the use of additional cumulants having little effect on the fit's statistical merit. Based on our previous experience, if any spectrum had had a double-exponential form, further increases in the number of cumulants used in the fit (as to four, five, ...) should have caused substantial improvements in the fit's statistical merit. The above data, taken with a 144-channel correlator and typical S/N of 300–400, therefore do not show two distinct groups of relaxations.

At fixed c, the variance $V = K_2^{1/2}/K_1$ had little dependence on I_b, changing by no more than 0.1 over the full ionic strength range. From the spectra used to obtain Figures 2 and 3, V at c = 5 g/L is 0.2–0.3 larger than at c = 1 g/L. As would be expected from the increase in V, spectra at c = 1 were fit well by two cumulants, while spectra for c = 5 g/L required three cumulants. The spectra used to generate Figure 1 reveal that V increases progressively with increasing c, the change in V over c = 0–5 g/L being 0.1 to (at I = 0.1 M) 0.3. Such changes in V are substantially larger than the point-to-point reproducibility of V in a single series of measurements.

Table II
Parameters from Nonlinear Least Squares Adjustments of the Stretched Exponential Form $D = D_0 \exp(\alpha I^\beta)$ to Measurements (Figures 2 and 3) of D against I at Fixed c, for Varying Fractions A of Polymer Neutralization[a]

model	c	A	D_0	α	β	rms error
i	0.93	1	1.08	0.053	−0.53	4%
	0.93	0.85	1.00	0.0104	−0.87	2%
	0.93	0.6	1.023	0.0123	−0.783	3%
	4.6	0.6	0.476	0.138	−2.43	5.5%
ii	0.93	1	1.67	0.41	−0.17	4%
	0.93	1	[1.10]	0.094	−0.35	4.5%
	0.93	0.85	1.10	0.0586	−0.45	2%
	0.93	0.6	1.11	0.0513	−0.46	3%
	4.6	0.6	0.32	1.5×10^{-4}	−0.45	5%
iii	0.93	1	0.969	0.0114	−0.84	3.5%
	0.93	0.85	0.997	9.8×10^{-3}	−0.88	2%
	0.93	0.6	1.098	0.0477	−0.47	3%
	0.93	0.6	[1.00]	7.3×10^{-3}	−0.89	3%
	4.6	0.6	0.34	5.6×10^{-4}	−2.41	2%
	4.6	0.6	0.515	0.0848	[−0.85]	6%
	4.6	0.6	[0.32]	6.8×10^{-5}	−3.09	5%

[a] Brackets indicate parameters which were held fixed, rather than being allowed to vary. Model numbers (first column) refer to different assumptions as to the contribution of the neutralized polymer (sodium polyacrylate) to I.

In the absence of polymer, counterion friction has a weak effect on D. We found that as I is increased from 0 to 0.02 to 0.1 M, D of the 0.038 μm spheres increases from 1.15×10^{-7} to 1.21×10^{-7} to 1.20×10^{-7} cm^2/s, respectively, D being virtually constant above 0.02 M.

pH and Probe Radius Effects. A preliminary survey, limited to I_b = 0 and I_b = 0.1 M, was made of the effect of pH and probe size on D. Figure 4 (and supplementary material, Table 9) shows D and R_{ap} for 0.93 g/L polyacrylic acid in pure water (added base, no added salt). The pH varied from 3.7 (corresponding to nonneutralized polymer) to 8. Over this pH range, η increases from 2.16 to 15.6 cP. In the same pH range, D of all spheres sizes first falls rapidly with increasing pH and then, for pH >5, tends to a constant. The dependence of D on pH increases with increasing sphere size. For the 0.7-μm spheres, D changes by more than a factor of 3 between pH 4 and 8, while D of the 0.038-μm spheres drops by only 50%. R_{ap} also falls with increasing solution basicity. In every mixture, R_{ap} is substantially smaller than R_0; i.e., diffusion is uniformly more rapid than expected from η and R_0. The 1.28-μm spheres gave erratic results under these conditions, so data points for them are not included in Figure 4.

D and R_{ap} for polystyrene spheres in 0.93 g/L poly(acrylic acid)/0.1 M NaCl are shown in parts a and b of Figure 5, respectively, (supplementary material, Table 10). Over the observed pH range, η increases from 1.38 to 1.7 cP. Over this pH range, D is constant for the larger spheres but increases substantially for the smaller spheres. R_{ap} of all spheres falls with increasing pH. At pH 4, all spheres have R_{ap}/R_0 substantially larger than unity. In more basic solutions, R_{ap} for the 0.7- and 1.28-μm spheres is close to R_0. At high pH, the 0.038-μm spheres have R_{ap} perhaps 25% less than R_0, while R_{ap}/R_0 of the 0.12-μm spheres declines to about 0.8.

Figure 6 (supplementary material, Table 11) presents D and R_{ap} for spheres in 4.6 g/L poly(acrylic acid) in solutions with I = 0. Data at pH 3.2 refers to nonneutralized

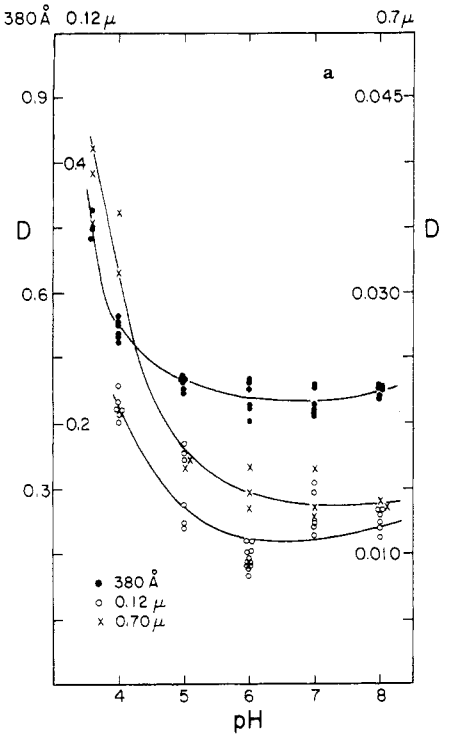

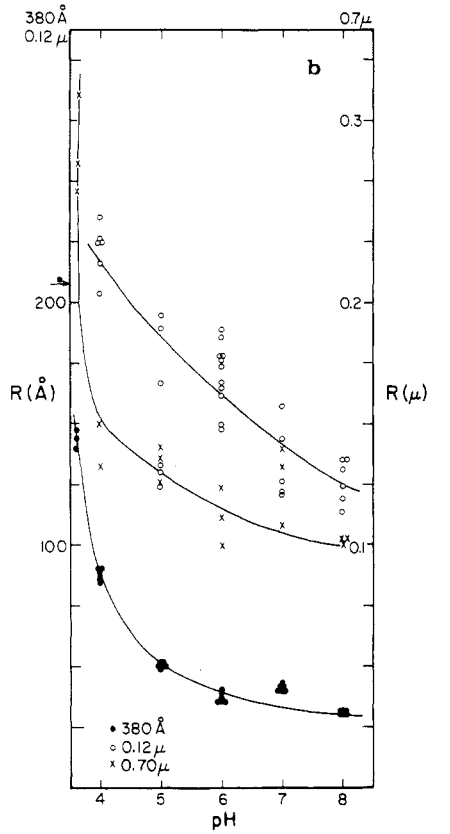

Figure 4. (a) D and (b) R_{ap} for 0.038, 0.12, and 0.70-μm spheres in 0.93 g/L poly(acrylic acid) in solutions containing no background electrolyte. D has units 10^{-7} cm^2/s. Note the use of different ordinate scales for the four sphere sizes. Horizontal arrow (b) indicates R_0 for the corresponding sphere species. The solid lines are trends and do not represent analytic functions.

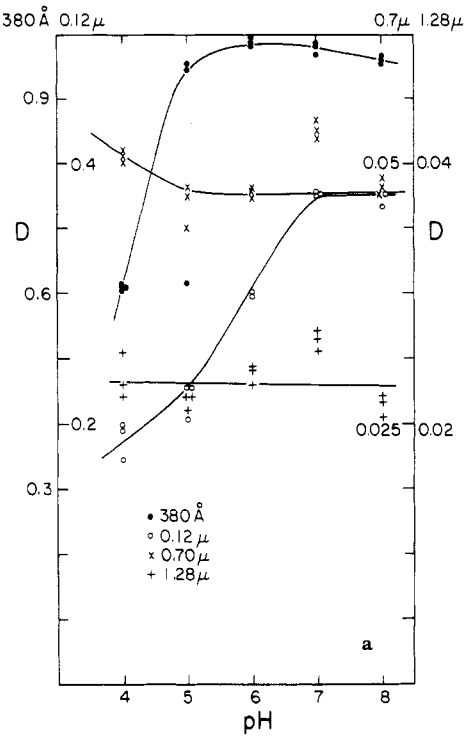

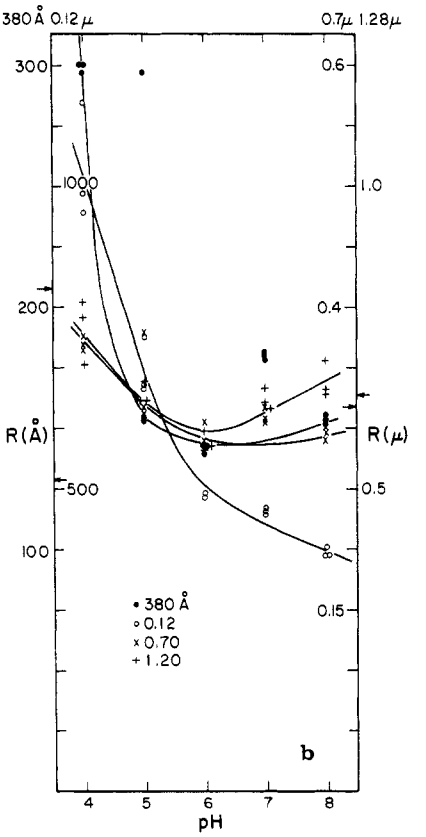

Figure 5. (a) D and (b) R_{ap} for 0.038-, 0.12-, 0.170-, and 1.28-μm spheres in 0.93 g/L poly(acrylic acid)/0.1 M NaCl. D has units 10^{-7} cm^2/s. Note the use of multiple ordinate scales. Other details are as in Figure 4.

polymer. Between pH 3.2 and 8, η increases from 2.8 to 67.6 cP, while D of each sphere type falls with increasing pH. For the two smaller spheres, D changes by 50% in 5 pH units. D of the larger spheres plunges dramatically between pH 3.2 and 6. The correlation between D and η is revealed in Figure 6b, which shows R_{ap} against pH. R_{ap} of the two smaller spheres depends strongly on pH. At pH 3.2, R_{ap}/R_0 of the 0.038-μm spheres is $\simeq$1.4. At pH 6–8, R_{ap}/R_0 is 0.12–0.14 for the 0.038-μm spheres and roughly 0.2 for the 0.12-μm spheres. In contrast to the behavior of the smaller spheres, R_{ap} of the larger spheres depends weakly on pH. In acidic solutions, R_{ap}/R_0 of the larger spheres is $\simeq$1, while in neutral solutions, R_{ap}/R_0 is

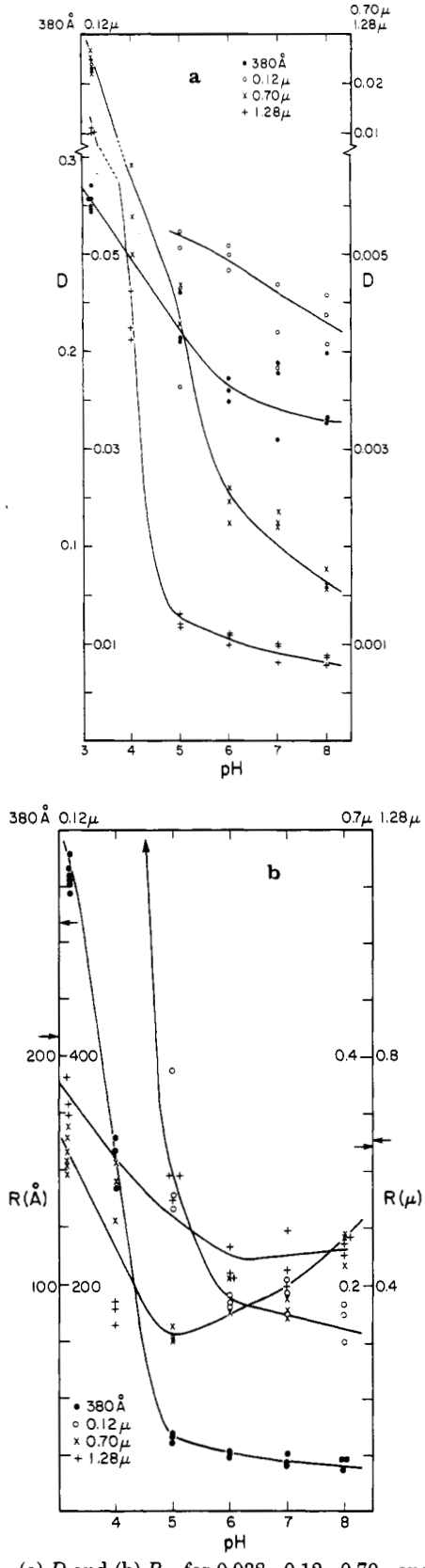

Figure 6. (a) D and (b) R_{ap} for 0.038-, 0.12-, 0.70-, and 1.28-μm spheres in 4.7 g/L poly(acrylic acid) in a solution containing no background electrolyte. D has units 10^{-7} cm^2/s. Note the use of multiple ordinate scales. Other details are as in Figure 4.

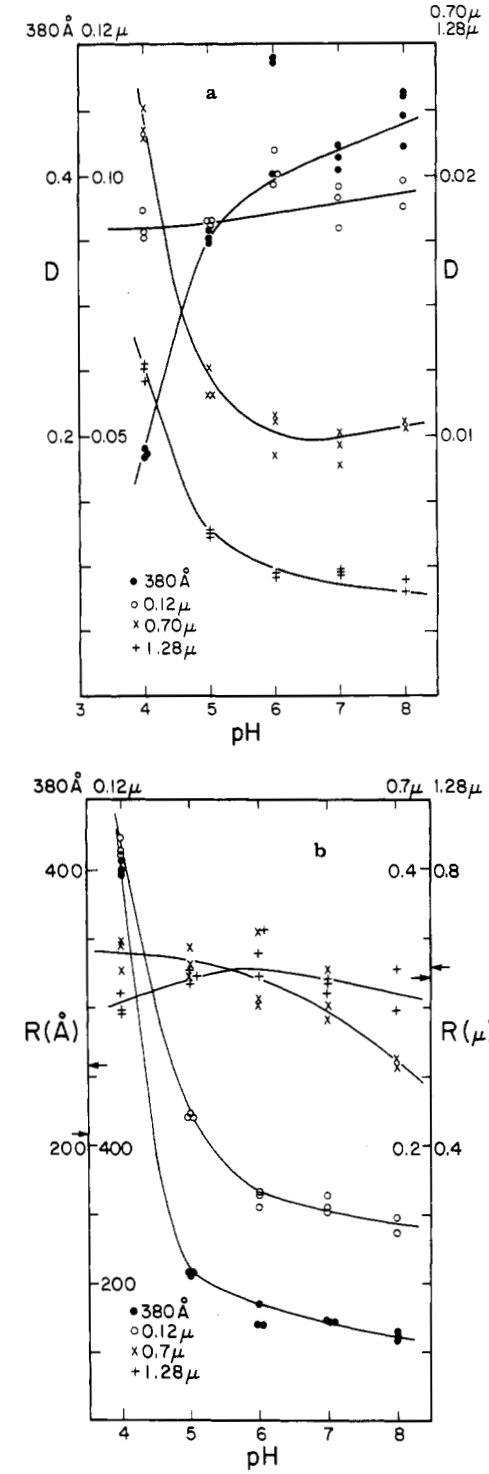

Figure 7. (a) D and (b) R_{ap} for 0.038-, 0.12-, 0.70-, and 1.28-μm spheres in 4.7 g/L poly(acrylic acid)/0.1 M NaCl. D has units 10^{-7} cm^2/s. Note the use of multiple ordinate scales. Other details are as in Figure 4.

$\simeq$0.6. In neutral solution, the validity of the Stokes–Einstein equation increases with increasing R but is not valid for any R studied.

D and R_{ap} for polystyrene spheres in 4.6 g/L poly(acrylic acid)/0.1 M NaCl appear in Figure 7 (supplementary material, Table 12). These solutions range from 3.1 to 8.5 cP in viscosity, η increasing as solutions are made more basic. The addition of salt made these solutions less than one-fifth as viscous as shown in Figure 6. Figure 7a shows the diffusion coefficients. For the smallest spheres, D increases with increasing pH. This trend reverses itself with the larger spheres. For 0.12-μm spheres, D is nearly independent of pH, while for the large spheres, D falls two- or threefold between pH 4 and 8. Figure 7b shows R_{ap} for the same spheres. R_{ap} falls very sharply with increasing pH for the smaller spheres, R_{ap}/R_0 reaching 0.3 for the 0.038-μm spheres and 0.6 for the 0.12-μm spheres. For the

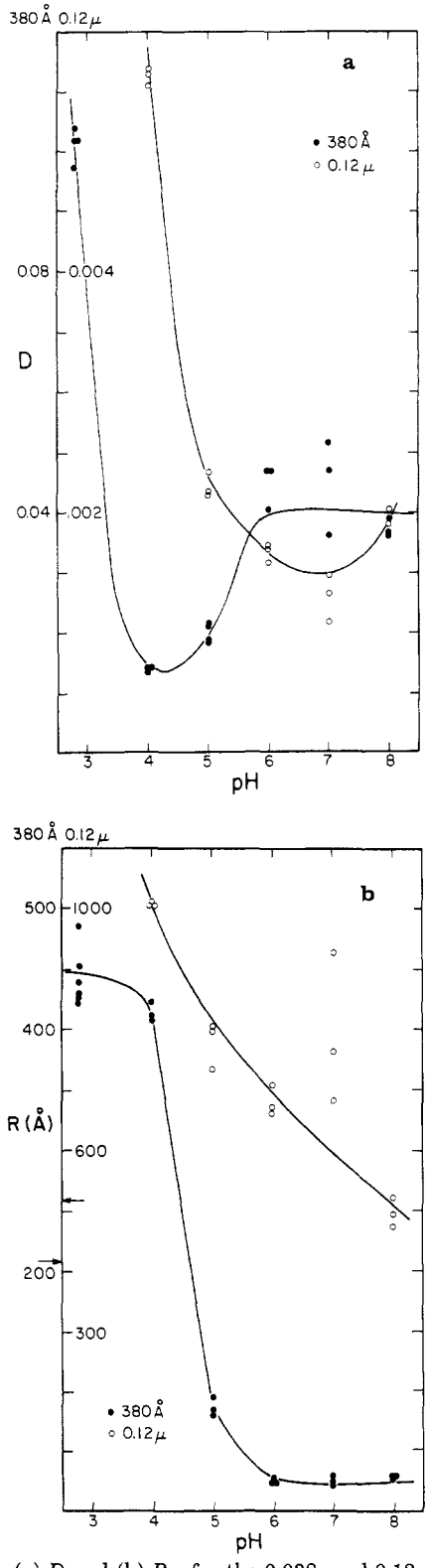

Figure 8. (a) D and (b) R_{ap} for the 0.038- and 0.12-μm spheres in 18.6 g/L polymer solution at various pH values. No background electrolyte was present. D has units 10^{-7} cm^2/s. Note the use of multiple ordinate scales. Other details are as in Figure 4.

larger spheres R_{ap}, which is nearly independent of pH, is not substantially different from R_0. In neutral solutions the Stokes–Einstein equation is again less accurate for small than for large spheres. However, from Figures 6 and 7 the addition of salt at fixed c improves the validity of eq 3.

Figure 8 (supplementary material, Table 13) shows D and R_{ap} in 20 g/L polymer solutions, with no added salt.

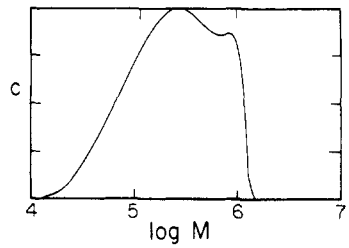

Figure 9. Molecular weight distribution of the poly(acrylic acid) obtained with size-exclusion chromatography, as described in ref 11.

pH 2.77 corresponds to nonneutralized poly(acrylic acid). These solutions are highly viscous (4.97–267 cP) and difficult to handle; individual values of D are much more scattered than would be the case in pure water. Measurements on the 0.7-μm spheres, which appear in the supplementary tables, obtained D values at the lower limit of resolution and are therefore not discussed here. D is substantially larger with nonneutralized than with neutralized polymers. For pH $\geq$6 (and hence $A \geq 0.5$) D and η both reach pH-independent plateaus. The connection between D and pH is more complicated than the connection between R_{ap} and pH. With increasing pH, D can show clear minima. However, with increasing pH, R_{ap} always falls, the fractional fall being larger for the smaller spheres. In neutral solution the 0.038-μm spheres diffuse much faster than expected from the Stokes–Einstein equation, while the 0.12-μm spheres diffuse slightly more slowly than expected.

Figures 4b–8b reveal the extent of validity of the Stokes–Einstein relation. K (or R_{ap}/R_0) falls with increasing pH, so that failures of eq 2 become more evident as the polymer charge density is increased. Furthermore, K is closer to unity at $I = 0.1$ than at $I = 0$, so eq 2 is more accurate when electrostatic forces are relatively short ranged. Finally, in the systems studied here, the Stokes–Einstein equation is more nearly valid for large than for small particles.

Our results on the Stokes–Einstein equation are consistent with previous studies by Lin and Phillies,[4-6] who observed probe diffusion in nonneutralized polyacrylic acid ($A = 0$) containing no added salt ($I = 0$). References 4–6 report that K (eq 3) decreases slightly with increasing sphere size. This trend of ref 4–6 is contrary to most of the data in Figures 4–8, which show that K increases with increasing R. However, nonneutralized poly(acrylic acid) solutions are quite acid (pH <4), so data points for Lin and Phillies' results would lie at the left margin of Figures 4–8. In nonneutralized salt-free polymer solutions, we find that K either is independent of sphere size (1, 20 g/L) or falls with increasing sphere radius (5 g/L), exactly as in ref 4–6.

Figure 9 shows the measured molecular weight distribution of the poly(acrylic acid). The wide distribution is typical of the systems through which biopolymer diffusion occurs in biological systems. For this system, M_n is 156 000 while M_w is 596 000. Almost all of the material in the sample has M larger than typical molecular weights for polymer entanglement.

Discussion

Our experimental data are most directly comparable with those of Gorti and Ware,[10] who used fluorescence photobleaching recovery to measure the diffusion of fluorescein, fluorescein-tagged serum albumin, and fluorescein-tagged polystyrene latex through polystyrene sulfonate solutions. In both studies, $D(c)$ is well described

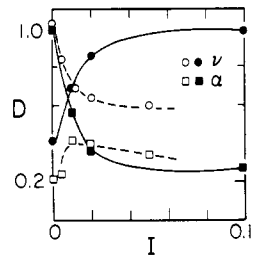

Figure 10. α (squares) and ν (circles), as functions of solution ionic strength, from fits of D (Figure 1) to $D = D_0 \exp(-\alpha c^{\nu})$. Filled circles are our results on polystyrene latex in poly(acrylic acid)/water; open circles are Gorti and Ware's data (10) on polystyrene latex in polystyrene sulfonate/water.

by the stretched exponential of eq 6. The two studies disagree as to the effect of I_b on α and ν. As seen in Figure 10, we find that α decreases monotonically with increasing I_b, while ν increases monotonically. In contrast, Gorti and Ware[10] report $d\alpha/dI > 0$ and $d\nu/dI < 0$. Comparing the basic data (Figure 1 of each paper) traces this discrepancy to the different behaviors observed for D at low concentration. We find D always increases with increasing I, while in Gorti and Ware's data there is a narrow region (roughly between 1 and 2 g/L of polymer) in which D falls with increasing I. At higher polymer concentrations, our work and ref 10 agree that $dD/dI > 0$. We also find that D falls sharply with decreasing I_b, while Gorti and Ware found (for $0.05 < c < 20$ g/L polystyrene sulphonate) that D is not affected by the presence of 0–0.05 M PO_4 buffer.

The Stokes–Einstein equation generally does not work in our systems. K is usually less than 1. This result does not appear to be an artifact. Probe aggregation or polymer adsorption by the probes would lead to $K > 1$, not $K < 1$. (We do observe $K > 1$ for the smallest spheres in the most acid solutions, precisely the conditions for the most noticeable polymer adsorption.) Accidental heterodyne detection, as might be caused by unrecognized immobile bodies in the scattering volume, could give an apparent $K \neq 1$. However, accidental heterodyning of the scattered light could only change K by twofold.

An artifact which could in principle explain the non-Stokes–Einsteinian behavior is *incomplete mixing*, in which the polystyrene spheres remain in void spaces containing solvent but little polymer, while the polymer is present at high concentration in regions containing few spheres. Such spatial inhomogeneities could be created by insufficient stirring after adding the polystyrene latex suspensions to polymer solutions. As time passed, solvent/polymer interdiffusion should diminish the inhomogeneities, so that D would fall with time. No such time dependence of D was seen, at least over 4–24-h intervals. Solvent-filled void spaces in solutions of long-chain entangling polymers could, of course, be argued to have long-term stability, so that they could persist over a 24-h period. However, we previously found $K < 1$ for probes in the nonentangling protein bovine serum albumin. The mutual diffusion coefficient of BSA at large c is known. In the probe/BSA system, interdiffusion would destroy even macroscopic (size-of-scattering-volume) voids before such voids could create a $K < 1$ effect. The findings in this paper are thus no different than findings in the BSA system in which the hypothesized voids certainly do not exist. We conclude that $K < 1$ is a physical phenomenon.

D and R_{ap} show a complicated set of dependencies on c, R, and pH. We note a simple (probably nonunique) model which predicts our observations:

First, the spheres can adsorb nonneutralized poly(acrylic acid), probably through hydrogen bonds between unionized carboxylic acid groups on the spheres and polymer chains. Making the solution more basic ionizes the carboxyl groups, reducing potential hydrogen bonding and increasing electrostatic polymer–sphere repulsions, so polyacrylic acid adsorption should be maximal at pH 2–4 and decrease at pH 6–8. Furthermore, polymer adsorption increases R_{ap} of different-sized spheres by similar amounts, having the largest fractional effect on R_{ap} of the small spheres, so polymer adsorption should be most apparent with the 0.038-μm spheres and least apparent with the 1.28-μm spheres. These expectations are confirmed by our data, in which R_{ap} of the small spheres falls sharply between pH 4 and 6, while R_{ap} of the large spheres is only weakly dependent on pH.

Second, non-Stokes–Einsteninian effects show a simple dependence on sphere size, ionic strength, and pH. In acidic solutions, the behavior of K is obscured by polymer adsorption. In basic solutions, K is less than unity for small spheres but increases toward unity with increasing sphere size. K is reduced if the electrostatic polymer–probe forces are increased, either by reducing the salt concentration or by increasing the polymer charge. Such trends are most apparent in the 4.6 g/L solutions (Figures 6b and 7b). These dependences of K, together with the measured behavior of η and polymer binding, qualitatively explain all the major features of Figures 4–8.

Theoretical models possibly relevant to our findings include calculations by Ogston et al.,[25] Langevin and Rondelez,[26] Altenberger and Tirrell,[27] and Cukier,[28] as well as the scaling analyses of polyeletrolyte systems by Odijk.[30] The calculations use very different assumptions as to the dominant physical forces in probe diffusion, though all refer to systems in which electrostatic interactions are not significant. All models link D/D_0 to a concentration-dependent parameter k, k^{-1} being a representative distance between polymer chains, but the rationales leading to k are different in different models. Altenberger and Tirrell[27] and Cukier[28] treat hydrodynamic probe–polymer interactions, while the model of Ogston et al.[25] involves the random placement of blocking obstacles in the probe's path. Langevin and Rondelez[26] present a scaling-model argument, based on the supposition that the behavior of D is known in several limits. The calculations predict forms like

$$D/D_0 = 1 - kR = \exp(-kR) \tag{8}$$

The models carry a common mnemonic image, a probe in a polymer solution being envisioned as a fish in a random net. If the probe ("fish") size R is much smaller than the mean distance between polymer chains (the mesh size of the net) k^{-1}, the probe diffuses ("swims") freely, so $D = D_0$. Probes whose size is comparable to the nearest polymer–polymer distance, like fish in a net whose mesh spacing satisfies $kR \simeq 1$, have their motions restricted by the net, so $D/D_0 < 1$. Several of the models predict k to be independent of polymer molecular weight, a result given by in the mnemonic: a fish is affected by the size of the holes in the net but not by the length of the ropes used to weave the net.

Optical probe studies[1-8] find that these models are not entirely successful when electrostatic forces are weak. D/D_0 follows a stretched-exponential form, which is like eq 8 if $k \simeq c^{\upsilon}$. υ is usually in the predicted range 0.5–1.0. However, in terms of eq 1 the models predict $\delta = 1$, $\gamma = 0$, while experiment[1-8] finds $\delta = 0$, $\gamma = 1$.

It is important to recall the concentration regimes in which these models may be valid. The calculations of Cukier[28] and Altenberger and Tirrell[27] treat probes interacting with pointlike obstacles. The results in ref 28,

while including semidilute concentrations, also apply at low concentration; ref 27 treats a limiting law ($c \rightarrow 0$) behavior. In contrast, the models of Ogston et al.[25] and Langevin and Rondelez[26] refer specifically to interwined polymer chains; i.e., they refer only to polymer concentrations in the so-called semidilute regime ($c > c^*$).

Are our solutions entangled? If poly(acrylic acid) were similar to polystyrene (i.e., if it were a random-coil polymer in a good solvent), then after correction for the difference in monomer molecular weights c^* would be near 20 g/L for our M. Neutralized poly(acrylic acid), especially in the absence of added salt, should be more rodlike than a neutral polymer, implying that neutralized PAA would have a smaller c^* than a polystyrene of comparable M. The viscosity of a pH 6 salt-free PAA solution (cf. supplementary tables 9–13) increases from 12.2 cP at 0.93 g/L to 55.6 cP at 4.65 g/L. If entanglement is taken to be revealed by a large increase in n with increasing c, then our 4.65 g/L solutions are entangled.

It should be recognized that c^* has generally been treated only for nonpolyelectrolytes, not for the charged polymers studied here. The common definition $c^* = a/[\eta]$ (for a in the range 1–4) implies that η is analytic in c, so that $[\eta] = \lim [(\eta - \eta_0)/\eta_0]$ is well defined. For $c < 1$ g/L the viscosity of nonneutralized, salt-free polyacrylic acid satisfies[29] $\eta = \eta_0 + ac^{1/2}$, so that $[\eta] = \infty$ and (formally) $c^* = 0$ (these anomalies are well-known polyelectrolyte effects). Application of the dilute/semidilute dichotomy to polyelectrolyte systems can thus lead to inclarities. Our data nonetheless indicate that at least some of our systems were entangled, while some of the theories predicting eq 8 are valid below as well as above c^*. We therefore attempt to compare eq 8 with our data.

These models need extension before application to systems with strong Coulomb forces. Gorti and Ware[10] began from Langevin and Rondelez's form[26] for semidilute solutions

$$D/D_0 = \exp[-(R/\xi)^\delta] + (\eta_0/\eta) \tag{9}$$

Here $\xi = k^{-1}$ is de Gennes' correlation length and η_0 is the solvent viscosity. To apply eq 9 to polyelectrolyte solutions, an expression for ξ is required. Gorti and Ware used Odijk's equation[30]

$$\xi \cong L_t^{-1/4} k_D^{1/4} (Ac)^{-3/4} \tag{10}$$

where L_t is the total persistence length, including the contribution of electrostatic repulsions within the chain, and k_D is the Debye screening length. For rods stiffened primarily by electrostatic interactions, eq 10 becomes[30]

$$\xi \cong Q^{1/4} k_D^{3/4} (Ac)^{-3/4} \tag{11}$$

Here $Q = e^2/\epsilon k_B T$ is the Bjerrum length, ϵ being the local dielectric constant; Q and k_D are related by $k_D^2 = 8\pi QI$, where I is the ionic strength of the solution. Substitution of eq 9 or 10 into eq 8 suggests the scaling law

$$D/D_0 = \exp(a(Rc^\nu A^\nu I^\beta M^\gamma)^\delta) + \eta_0/\eta \tag{12}$$

The theories predict $\delta = 1$, $\gamma = 0$, $\nu = {}^3/_4$, and $\beta = -0.375$.

Equations 9–12 motivated us to describe ionic strength dependences with a stretched exponential

$$D/D_0 = \exp(+\alpha I^\beta) \tag{13}$$

To compare eq 13 with experiment, a value for I is needed. I includes added NaCl; it could also include the polyacrylate salt. Four obvious phenomenological definitions of I would (i) include only the NaCl, (ii) include all mobile ions, including the Na^+ used to neutralize the polymer, (iii) include all ions in solution, with each acrylate group counted as a separate monovalent ion, or (iv) include all ions in solution, the polyacrylate polyion being treated as a single macroion of charge $-Z$. Alternative iv predicts I to be very large ($\sim 10^5$ M, assuming $Z_{PAA} \sim 3000$) and practically independent of I_b, contrary to the observed strong dependence of D on I_b.

Measurements for each pH and c were fit separately to eq 13, using definitions i, ii, and iii for I, to obtain Table II. Alternative iii, which finds $\beta \approx -0.8$ to -0.9, gives the most consistent results. Alternative iii is also the most consistent with the Debye–Huckel model, in that model i neglects the screening effect of intervening polymers on polymer–polymer interactions, while model ii formally contains an unequal number of anions and cations, contrary to the mathematical assumptions of the Debye–Huckel calculation. $\beta = -0.9$ differs twofold from expectations related to eq 12. Equation 12 does, however, give a reasonable form for the relation between and A; the observed $\alpha \sim A^1$ (Table II, case iii) is not too dissimilar to the prediction $\nu = {}^3/_4$.

There is an interesting coincidence between the dependence of α (eq 6) on M and I. The observed $\alpha \sim M^{0.8}$ for neutral polymers is equivalent to $\alpha \sim 1/c^*$ (since $c^* \sim M^{1-3\nu}$); i.e., with c in molar units for neutral polymers, α is proportional to the volume v^* effectively occupied by a single polymer chain. For a charged rodlike polymer chain, v^* is proportional to Mk_D^2, M being the length of the polymer chain and $1/k_D$ being the chain's *effective* lateral dimension. If α for polyelectrolytes were $\sim v^*$, then $\alpha \sim I^{-1}$ would be expected. This expectation is in good agreement with the observed $\alpha \sim I^{-0.9}$ implying for polyelectrolytes $\alpha \sim M^1$ with c in molar units. (Our data do not test this prediction.)

D (Figure 4–8) at pH 7 and fixed c was also fit to

$$D/D_0 = \exp(-KR^\delta) \tag{14}$$

with K and δ as free parameters. At $c = 1$ g/L, $\delta \sim 0$ in the absence of salt, but $\delta \sim 0.3$ at $I = 0.1$ M. With 5 g/L polymer, eq 14 fits the data poorly (two parameters for four data points resulting in root mean square errors of 16–18%); the forced fit finds $\delta = 0.16$–0.19. Our values for δ are midway between values for probes in neutral polymer solutions (where $\delta \cong 0 \pm 0.2$), and Gorti and Ware's data on probe–polyelectrolyte mixtures (where $\delta = 0.5 \pm 0.25$). The theoretical estimate $\delta = 1$, based on eq 8 and its extension, leads to an order-of-magnitude error in predicting D/D_0.

The arguments[26] for eq 9 assumed that the Stokes–Einstein equation should be valid for sufficiently large particles, contrary to our experimental finding $K < 1$ for micron-size particles. The assumption arises from (i) Einstein's computation of D from sedimentation-diffusion equilibrium, which yields

$$D = k_B T/f \tag{15}$$

and (ii) the common expectation that Stokes' Law is valid for macroscopic bodies. A body which is sufficiently large that the solvent can be approximated as a continuum is usually said to be "macroscopic". However, polymer solutions are often non-Newtonian; in a polymer solution Stokes' law need not be valid. The apparent viscosity obtained with a falling-ball viscometer may depend on the ball's rate of fall. If Stokes' law is inapplicable, eq 15 does not imply the Stokes–Einstein equation.

Our measurements of D and η are not inconsistent with eq 15. Einstein's argument shows that the drag coefficient f_D inferred from D equals the drag coefficient f_s inferred from the sedimentation of the same body. f_s describes the resistance to sedimentation of a body which is simulta-

neously performing Brownian ("jittering") motion. Non-Newtonian systems often show nonlinear hydrodynamics. If the motion of a body has two velocity components, the total drag on that body in a non-Newtonian fluid may not be the sum of the drags experienced if the body performed each of the component motions separately. The sedimentation of a Brownian particle need not be the same as the sedimentation of an elsewise similar particle whose Brownian motion has been suppressed. Einstein's arguments refer to the drag coefficient of a particle which simultaneously sediments and diffuses, not to a body which sediments without undergoing Brownian motion.

In conclusion, we have observed probe diffusion in a polyelectrolyte solution, noting the dependence of D on the major experimental variables: polymer concentration, polymer neutralization, ionic strength, probe radius, and solution viscosity. Relatively simple relations connect these variables. The available theoretical models for D are not entirely satisfactory, in that they predict incorrectly the dependence of D/D_0 on R and do not predict accurately the dependence of D on I or c. Identification of the relationship between D and viscosity requires a more extensive study of the rheological properties of the polyelectrolyte solutions used for the probe diffusion measurements.

Registry No. Polystyrene, 9003-53-6; poly(acrylic acid) sodium salt, 9003-04-7.

Supplementary Material Available: Tables of D values for polystyrene spheres at various electrolyte concentrations as a function of polymer concentration and at various pHs and polymer concentrations as a function of the concentration of added NaCl and tables of results at various pHs on polystyrene spheres in different poly(acrylic acid) and NaCl concentrations (13 pages). Ordering information is given on any current masthead page.

References and Notes

(1) Ullmann, G. S.; Phillies, G. D. J. *Macromolecules* **1983**, *16*, 1947.
(2) Ullmann, G. S.; Ullmann, K.; Lindner, R.; Phillies, G. D. J. *J. Phys. Chem.* **1985**, *89*, 692.
(3) Phillies, G. D. J. *Biopolymers* **1985**, *24*, 379.
(4) Lin, T. H.; Phillies, G. D. J. *J. Phys. Chem.* **1982**, *86*, 4073.
(5) Lin, T.-H.; Phillies, G. D. J. *J. Colloid Interface Sci.* **1984**, *100*, 82.
(6) Lin, T.-H., Phillies, G. D. J. *Macromolecules* **1984**, *17*, 1686.
(7) Ullmann, K.; Ullmann, G. S.; Phillies, G. D. J. *J. Colloid Interface Sci.* **1985**, *105*, 315.
(8) Phillies, G. D. J.; Ullmann, G. S.; Ullmann, K.; Lin, T.-H. *J. Chem. Phys.* **1985**, *82*, 5242.
(9) Phillies, G. D. J. *Macromolecules* **1986**, *19*, 2367.
(10) Gorti, S.; Ware, B. R. *J. Chem. Phys.* **1985**, *83*, 6449.
(11) Callec, G.; Anderson, A. W.; Tsao, G. T.; Rollings, J. E. *J. Appl. Polym. Sci.* **1984**, *22*, 287.
(12) Kato, Y.; Komiya, Y.; Iwaeda, T.; Sasaki, H.; Hashimato, T. *J. Chromatogr.* **1981**, *208*, 105; *206*, 135; *208*, 71; *211*, 383.
(13) Yau, W. W.; Kirkland, J. J.; Bly, D. D. *Modern Size-Exclusion Chromatography*; Wiley: New York, 1975, p 61.
(14) McConnell, M. L. *Am. Lab.* **1978**, *10* (5), 63.
(15) Ouano, A. C.; Kaye, W. *J. Polym. Sci.* **1974**, *12*, 1151.
(16) Yu, L.-P., Rollings, J. E. *J. Appl. Polym. Sci.* **1987**, *33*, 1909.
(17) Gorti, S.; Plank, L.; Ware, B. R. *J. Chem. Phys.* **1984**, *81*, 909.
(18) Koppell, D. E. *J. Chem. Phys.* **1972**, *57*, 4814.
(19) Phillies, G. D. J. *J. Chem. Phys.* **1974**, *60*, 983.
(20) Phillies, G. D. J. *Macromolecules* **1976**, *9*, 447.
(21) Jones, R. B. *Physica* **1979**, *97A*, 113.
(22) Kops-Werkhoven, M.-M.; Pathmamanoharan, C.; Vrij, A.; Firjnaut, H. M. *J. Chem. Phys.* **1982**, *77*, 5913.
(23) Lodge, J. P. *Macromolecules* **1983**, *16*, 1393.
(24) Noggle, J. H. *Physical Chemistry on a Microcomputer*; Little, Brown, and Co.: New York, 1985.
(25) Ogston, A. G.; Preston, P. N.; Wells, J. D. *Proc. R. Soc. London, A* **1973**, *333*, 297.
(26) Langevin, D.; Rondelez, F. *Polymer* **1978**, *14*, 875.
(27) Altenberger, A. R.; Tirrell, M. *J. Chem. Phys.* **1984**, *80*, 2208.
(28) Cukier, R. I. *Macromolecules* **1984**, *17*, 252.
(29) Malone, C. M.S. Thesis, Worcester Polytechnic Institute, 1986.
(30) Odijk, T. *Macromolecules* **1974**, *12*, 688.

Reptation of Living Polymers: Dynamics of Entangled Polymers in the Presence of Reversible Chain-Scission Reactions

M. E. Cates

Institute for Theoretical Physics, University of California, Santa Barbara, California 93106.

Received December 12, 1986

ABSTRACT: A theoretical study is made of the dynamics of stress relaxation in a dense system of "living" polymers. These are linear chain polymers that can break and recombine on experimental time scales. A simple model for the reaction kinetics is assumed, in which (i) a chain can break with equal probability per unit time per unit length at all points in the chemical sequence and (ii) two chains can combine with a rate proportional to the product of their concentrations. The chain length distribution is then exponential with mean $\bar{L}$; $\bar{L}$ is taken to be large enough that $\alpha = L_e/\bar{L} \ll 1$, where L_e is the entanglement length. It is further assumed that stress relaxation proceeds by the reptation mechanism—a process that may, however, be abetted by the constant breaking and reforming of the chains (thus enhancing the rate at which portions of unrelaxed tube become first occupied by a chain end, causing them to relax). Two relevant time scales are τ_{rep}, the reptation time of a polymer of length $\bar{L}$, and $\tau_{break} \equiv \tau_{rep}\zeta$ (say) the mean time for such a chain to break into two pieces. For $\zeta \gtrsim 1$, the dominant stress-relaxation mechanism is simple reptation (with characteristic time τ_{rep}). For $\alpha \lesssim \zeta \lesssim 1$, it is predicted that stress relaxation is characterized by a new *intermediate* time scale, $\tau = \tau_{rep}\zeta^{1/2} = (\tau_{rep}\tau_{break})^{1/2}$, associated with a process whereby the chain breaks at a point close enough to a given segment of tube for reptative relaxation of that segment to occur before the new chain end is lost by recombination. Crossovers are ascribed to similar relaxation mechanisms involving the breathing modes of the chain and local Rouse-like motion, which dominate respectively when $\alpha^3 \lesssim \zeta \lesssim \alpha$ and $\zeta \lesssim \alpha^3$.

1. Reptation Model

The dynamical theory of polymer melts has advanced remarkably in recent years. It was first suggested by de Gennes[1a] that the chief relaxation mechanism, for long linear polymers in the melt, is that of reptation. This process consists in the gradual disengagement of any given chain, by curvilinear diffusion along its own contour, from a tubelike environment. The tube is made up of neighboring chains; these present a set of topological obstacles to diffusion normal to the chain contour (Figure 1). For chains of length L, the fundamental relaxation time of the system is then

$$\tau = \tau_{rep} = L^3/D_0 \quad (1)$$

0024-9297/87/2220-2289$01.50/0